Elucidation of Distinct Ligand Binding Sites for Cytochrome P450 3A4†

Natilie A. Hosea,‡ Grover P. Miller, and F. Peter Guengerich*

Department of Biochemistry and Center in Molecular Toxicology, Vanderbilt University School of Medicine, Nashville, Tennessee 37232-0146

Received December 2, 1999; Revised Manuscript Received February 10, 2000

ABSTRACT: Cytochrome P450 (P450) 3A4 is the most abundant human P450 enzyme and has broad selectivity for substrates. The enzyme can show marked catalytic regioselectivity and unusual patterns of homotropic and heterotropic cooperativity, for which several models have been proposed. Spectral titration studies indicated one binding site for the drug indinavir (M_r 614), a known substrate and inhibitor. Several C-terminal aminated peptides, including the model morphiceptin (YPFP-NH_2), bind with spectral changes indicative of Fe−NH_2 bonding. The binding of the YPFP-NH_2 N-terminal amine and the influence of C-terminal modification on binding argue that the entire molecule (M_r 521) fits within P450 3A4. YPFP-NH_2 was not oxidized by P450 3A4 but blocked binding of the substrates testosterone and midazolam, with K_i values similar to the spectral binding constant (K_s) for YPFP-NH_2. YPFP-NH_2 inhibited the oxidations of several typical P450 substrates with K_i values 10-fold greater than the K_s for binding YPFP-NH_2 and its K_i for inhibiting substrate binding. The *n* values for cooperativity of these oxidations were not altered by YPFP-NH_2. YPFP-NH_2 inhibited the oxidations of midazolam at two different positions (1′- and 4-) with 20-fold different K_i values. The differences in the K_i values for blocking the binding to ferric P450 3A4 and the oxidation of several substrates may be attributed to weaker binding of YPFP-NH_2 to ferrous P450 3A4 than to the ferric form. The ferrous protein can be considered a distinct form of the enzyme in binding and catalysis because many substrates (but not YPFP-NH_2) facilitate reduction of the ferric to ferrous enzyme. Our results with these peptides are considered in the context of several proposed models. A P450 3A4 model based on these peptide studies contains at least two and probably three distinct ligand sites, with testosterone and α-naphthoflavone occupying distinct sites. Midazolam appears to be able to bind to P450 3A4 in two modes, one corresponding to the testosterone binding mode and one postulated to reflect binding in a third site, distinct from both testosterone and α-naphthoflavone. The work with indinavir and YPFP-NH_2 also argues that room should be present in P450 3A4 to bind more than one smaller ligand in the "testosterone" site, although no direct evidence for such binding exists. Although this work with peptides provides evidence for the existence of multiple ligand binding sites, the results cannot be used to indicate their juxtaposition, which may vary through the catalytic cycle.

P450[1] 3A4 is the most abundant P450 in human liver and is also found at high levels in the intestinal tract (*3*−*5*). This enzyme oxidizes endogenous and exogenous compounds as well as over half of the drugs in therapeutic use (*5*). Although P450 3A4 is often characterized as possessing a broad substrate selectivity due to the structural diversity of these substrates, the enzyme has a distinct specificity as indicated by the regioselectivity and steroselectivity with its substrates (*5*, *6*). The mechanisms underlying the selectivity of a catalyst of this type are of interest in basic enzymology as well as for practical applications.

In previous reports, P450 3A4 has demonstrated non-Michaelis−Menten kinetics (homotropic cooperativity), and catalytic activity can be directly stimulated or inhibited by secondary ligands (heterotropic cooperativity) in some but not all reactions. Some of the first studies in this area involved P450 3A subfamily orthologues in experimental animals. Early work in the P450 field demonstrated the stimulation of various uncharacterized P450 activities in microsomes (*7*). The work of Conney and his associates with rabbit and human P450 systems can now be interpreted in terms of heterotropic stimulation of P450 3A enzymes by flavonoids and other compounds (*8*−*12*). Johnson proposed an allosteric model to explain homotropic phenomena seen with some oxidations catalyzed by P450 3A(6) (*13*). Studies with rats suggest the in vivo significance of these P450 3A effects, under a model in which the ligand caffeine affects acetaminophen oxidation (*14*). Both homotropic and hetero-

† This work was supported in part by U.S. Public Health Service (USPHS) Grants R35 CA44353 and P30 ES00267. N.A.H. is the recipient of USPHS postdoctoral fellowship F32 CA74492. G.P.M. is the recipient of USPHS postdoctoral fellowship F32 GM19808.

* Address correspondence to this author at the Department of Biochemistry, Vanderbilt University School of Medicine, 638 Medical Research Bldg. I, 23rd and Pierce Avenues, Nashville, TN 37232-0146. Telephone (615) 322-2261; Fax (615) 322-3141; email guengerich@toxicology.mc.vanderbilt.edu.

‡ Present address: Central Research Division, Pfizer, Inc., Eastern Point Rd., Groton, CT 06340.

[1] Abbreviations: P450, cytochrome P450 [also termed "heme-thiolate P450" by Enzyme Commission (EC 1.14.14.1) (*1*, *2*)]; ESI, electrospray ionization; MS, mass spectrometry; αNF, α-naphthoflavone (7,8-benzoflavone); CHAPS, 3-[(3-choloamidopropyl)-dimethylammonio]-1-propanesulfonic acid; HEPES, *N*-(2-hydroxyethylpiperazine)-*N*′-(2-ethanesulfonic acid).

10.1021/bi992765t CCC: $19.00
Published on Web 04/19/2000

tropic cooperativity (*15*) have been observed in recombinant P450 3A4 systems and several explanations have been proposed. These include multiple, ligand-dependent conformations (*16, 17*) and a single cavity in the binding site large enough to accommodate ≥2 ligands, which either compete for access to the heme iron (*18*−*20*) or fit in "head-to-tail" or "side-to-side" patterns to alter regioselectivity (*21, 22*). Complicating issues include the variability in heterotropic interactions often seen under varying conditions [e.g., buffer composition (*23*)] and the relatively low degree of positive cooperativity (e.g., Hill *n* values usually ≤ 1.3) (*6, 22, 24*−*26*).

In our own work with P450 3A4, αNF stimulated the 8,9-epoxidation of aflatoxin B_1 and attenuated its 3α-hydroxylation (*6*). Further, both reactions showed positive cooperativity in the absence of αNF ($n \sim 2.0$) and no cooperativity in the presence of αNF. This cooperativity is the strongest reported for a homogeneous P450 3A enzyme. Another interesting point is that patterns of regioselectivity of aflatoxin B_1 oxidation were very different when artificial oxygen surrogates (e.g., cumene hydroperoxide, iodosylbenzene) replaced the NADPH−P450 reductase system and no positive heterotropic cooperativity was observed (*6*). The pattern of homotropic cooperativity shows variation depending upon the reduction system used to deliver electrons to P450 3A4 (*6, 27*). Alternatively, others have proposed models that suggest a rather rigid P450 in which multiple ligands bind to yield the observed patterns of cooperativity (*20*−*22, 24, 28*). However, direct evidence of a ligand stoichiometry greater than unity for P450 3A4 has not been shown.

To address the issue of stoichiometry, we employed a variety of conventional binding techniques. All of the approaches relied on accurate quantitation of both bound and free species of enzyme. These ligand interaction techniques included gel-filtration approaches (*29*), equilibrium dialysis, and binding to immobilized P450 3A4 [attached through a C-terminal $(His)_5$-tag to Ni^{2+} resin]. None of these studies revealed conclusive evidence regarding the stoichiometry of binding, due to complications resulting from nonspecific binding components, which prevented the correction of binding data.

In continuing our studies, we exploited the binding and catalytic properties of peptides, including a peptide mimic, indinavir, to further examine the complex interligand interactions that typify studies of human P450 3A4. Many oligopeptides have important biological functions, e.g., neuropeptides, bradykinin, and enkephalins. P450 oxidation has not really been considered to play a major role in metabolism of peptides [with the notable exceptions of cyclosporin A (*30*) and bromocriptine (*31*)], although few studies have been done to explore this possibility. However, a major general approach to drug design and development is the identification of critical peptide regions in protein interactions and appropriate modification of the peptides to enhance drug response and bioavailability. Thus, interactions of relatively hydrophobic oligopeptides with P450s can be expected.

Our binding studies took advantage of the different shifts in the Soret spectrum resulting from binding interactions. Most P450 3A4 ligands induce a "type I" spectral shift (*32*) upon binding the enzyme, but several peptides and derivatives induce a "type II" spectral shift (*32, 33*) upon formation of the ligand-bound complex. To further examine the nature of the ligand-bound complex, we exploited the binding properties toward P450 3A4 of several peptides that had been examined and reported by Delaforge et al. (*34*). The effects of a variety of ligand combinations on the rate of formation of ferrous P450 (·CO complex) from ferric P450 were measured. Finally, steady-state analysis was performed for the classical P450 3A4 substrates testosterone, midazolam, and 17β-estradiol. Taken together, these studies provide evidence for a model for P450 3A4 with at least two and probably three binding sites with somewhat distinct features.

EXPERIMENTAL PROCEDURES

Chemicals. Testosterone, 6β-hydroxytestosterone, L-α-1,2-dilauroyl-*sn*-glycero-3-phosphocholine, L-α-dioleoyl-*sn*-glycero-3-phosphocholine, bovine brain phosphatidylserine, αNF, and most peptides were obtained from Sigma Chemical Co. (St. Louis, MO). The peptide YPFP was purchased from Bachem Bioscience (King of Prussia, PA). 17β-Estradiol, 2-hydroxylestradiol, and 4-hydroxylestradiol were obtained from Steraloids Inc. (Newport, RI). Midazolam, 1′-hydroxymidazolam, and 4-hydroxymidazolam were gifts from A. J. J. Wood, Vanderbilt University. Indinavir was generously provided by J. H. Lin (Merck, West Point, PA).

Synthesis of N-Acetyl-YPFP-NH₂. YPFP-NH_2 (25 mg) was dissolved in 1 mL of pyridine. A stoichiometric amount of acetic anhydride (ACS grade, 98%) to peptide was added; the mixture was incubated at room temperature for 30 min, at which time a stoichiometric amount of NH_4OH (in CH_3OH) was added. The reaction was evaporated to dryness with a Centrivap concentrator (Labconco, Kansas City, MO). The product was purified by HPLC on a Beckman ODS Ultrasphere octadecylsilane column (10 × 250 mm, Beckman, San Ramon, CA) under gradient conditions: H_2O/CH_3CN (86/14 v/v, containing 0.10% CF_3CO_2H) to H_2O/CH_3CN (68/32 v/v, containing 0.10% CF_3CO_2H) over 20 min, maintaining the latter condition for 5 min before returning to the initial conditions. The chromatography was monitored at 230 nm and peaks eluting at t_R 32.8 and 38.2 mL were recovered and dried under N_2. Samples were resuspended in a 50/50 mixture (v/v) of a CH_3OH/H_2O solution [containing 0.10% (v/v) CH_3CO_2H] and then subjected to ESI MS with a Finnigan TSQ 7000 spectrometer (Finnigan, Sunnyvale, CA) by flow infusion. Operating conditions were as follows: ion spray voltage, 4.0 kV; ion spray current, 1 μA; electron multiplier, 1300 V; mass range, *m*/*z* 50−750; N_2 sheath gas, 70 psi; ion source pressure, 845 mTorr; manifold pressure, 5.5×10^{-6} Torr; capillary voltage and temperature, 20 V and 230 °C; tubel voltage, 71.1 V; and detection under positive ion mode. Data were accumulated over each 1 min interval with scans taken every 1 s. The signals seen were *m*/*z* 522.4 for the peak eluting at 32.8 mL (indicative of YPFP-NH_2) and *m*/*z* 564.4 for the peak eluting at 38.2 mL (indicative of *N*-acetyl-YPFP-NH_2), with no starting material detected in the purified acetylation product.

Enzyme Preparations. Recombinant P450 3A4 containing a C-terminal $(His)_5$ tag was prepared from P450 3A4 (NF14) (*35, 36*) according to Domanski et al. (*22*). The construct was expressed in *Escherichia coli* DH5α and recovered from the membranes by solubilization of the P450 with CHAPS (1.0% w/v) instead of nonionic detergents (*37*). The P450 3A4 was purified by a two-step procedure: solubilized P450

was loaded onto a 2.5 × 10 cm DEAE-Sephacel column (Fast Flow, Pharmacia, Piscataway, NJ) equilibrated with 20 mM potassium phosphate buffer (pH 7.4) containing 20% glycerol (v/v) and 1.0% CHAPS (w/v). The flowthrough fraction was diluted with KCl (0.5 M final concentration) and loaded onto a 1.25 × 3 cm Ni^{2+}-nitrilotriacetate column (Qiagen, Valencia, CA) equilibrated with 20 mM potassium phosphate buffer (pH 7.4) containing 20% glycerol (v/v), 0.5% CHAPS (w/v), 0.5 M KCl, and 10 mM β-mercaptoethanol. The column was washed with 10 bed volumes of the equilibration buffer and then 10 bed volumes of equilibration buffer devoid of CHAPS. P450 3A4 was eluted with 20 mM potassium phosphate buffer (pH 7.4) containing 20% glycerol (v/v), 0.5 M KCl, 200 mM imidazole, and 10 mM β-mercaptoethanol (pH adjusted to 7.4 with 43% H_3PO_4). Colored fractions were pooled, dialyzed 3× vs 100 volumes of 10 mM potassium phosphate buffer (pH 7.4) containing 20% glycerol (v/v), 0.1 mM EDTA, and 0.1 mM dithiothreitol, and stored in aliquots at −20 °C.

The amount of P450 was determined spectrally (Fe^{2+}·CO vs Fe^{2+} spectra) by the method of Omura and Sato (*38*). Protein concentration was determined (following 24 h hydrolysis in 6 N HCl, 110 °C) in the Vanderbilt facility.

Recombinant rat NADPH−P450 reductase was expressed in *E. coli* and purified by the method of Shen et al. (*39*) as modified by Hanna et al. (*40*). Rabbit liver cytochrome b_5 was prepared as described previously (*41*).

P450 Catalytic Activity Assays. Purified P450 3A4 was reconstituted in batches with 0.5 μM P450, 1.0 μM NADPH−P450 reductase, 0.5 μM cytochrome b_5, and 0.5 mg of CHAPS mL^{-1} (0.8 mM), 0.10 mg of phospholipid mix mL^{-1} [1/1/1 (w/w/w) L-α-1,2-dilauroyl-*sn*-glycero-3-phosphocholine/L-α-dioleoyl-*sn*-glycero-3-phosphocholine/bovine brain phosphatidylserine], and 50 mM potassium HEPES (pH 7.4); aliquots were stored at −20 °C (for validation of premixes see ref *27*). Premixes (100 μL) were diluted 5-fold with 300 μL of H_2O and 100 μL of 5× premix buffer (200 mM potassium HEPES and 150 mM $MgCl_2$, pH 7.4) to 500 μL total volume. Ascorbic acid (1.0 mM final) was added to the 17β-estradiol oxidation reactions to minimize conversion of 2-hydroxyestradiol to the *o*-quinone. The reaction mixtures (after ligands were added) were incubated for 3 min at 37 °C, at which time reactions were initiated by addition of an NADPH-generating system [0.5 mM $NADP^+$, 1 IU of glucose 6-phosphate dehydrogenase mL^{-1}, and 10 mM glucose 6-phosphate (*42*)]. Peptides were dissolved in H_2O; other ligands were dissolved in CH_3OH. The final concentration of CH_3OH in reaction mixtures was ≤2% (v/v). After incubation at 37 °C for a designated time (testosterone, 5 min; midazolam, 17β-estradiol, and αNF, 10 min; YPFP-NH_2, 30 min), reactions were quenched with either 2 volumes (1 mL) of ethyl acetate plus 0.2 volume (100 μL) of a solution containing 1 M Na_2CO_3 and 2 M NaCl (pH 10.5) for testosterone, midazolam, and αNF, or 2 volumes of CH_2Cl_2 for 17β-estradiol. The samples were mixed with a vortex device for 10 s and the layers were separated by centrifugation at 450*g* for 10 min. The organic layer from each sample was transferred to a sample vial, dried under a N_2 stream, and dissolved in the mobile phase for HPLC. Reactions with the peptide, YPFP-NH_2, were quenched with 0.55 volume of 17% aqueous $HClO_4$ and then filtered through a centrifuge tube filter containing a 0.22 μM nylon membrane (Costar, Corning, NY).

The reaction products were resolved by HPLC on a Develosil ODS (4.6 × 150 mm) column (Nomura Chemical Co., Japan). The mobile phases and detection wavelengths were as follows: testosterone oxidation, H_2O/CH_3OH (30/70 v/v), detection at 254 nm; αNF oxidation, H_2O/CH_3OH (20/80 v/v), detection at 220 nm; midazolam oxidation, 10 mM potassium phosphate (pH 7.4)/CH_3OH/CH_3CN (40/38/22 v/v/v), detection at 220 nm. 17β-Estradiol oxidation gradient conditions were as follows: 0−5 min, 100% A; 5−7 min, 100% A to 100% B; 7−8 min, 100% B; 8−10 min, 100% B to 100% A; 10−12 min, 100% A, where A is H_2O/CH_3OH (40/60 v/v) containing 0.5% CH_3CO_2H (v/v) and B is H_2O/CH_3OH (10/90 v/v) containing 0.5% CH_3CO_2H (v/v). Oxidation of YPFP-NH_2 was assessed by HPLC/ESI/MS (TSQ 7000 spectrometer, Finnigan, Sunnyvale, CA); a 3.0 × 250 mm octadecylsilane Phenomenex column was used with a gradient of H_2O/CH_3OH (95/5 v/v, containing 10 μM $NH_4CH_3CO_2$) to H_2O/CH_3OH (5/95 v/v, containing 10 μM $NH_4CH_3CO_2$) over 30 min, stationary at H_2O/CH_3OH (5/95 v/v, containing 10 μM $NH_4CH_3CO_2$) over 20 min, returned to H_2O/CH_3OH (5/95 v/v, containing 10 μM $NH_4CH_3CO_2$) over 10 min. Operating conditions were as follows: ion spray voltage, 3.6 kV; ion spray current, 1.5 μA; electron multiplier, 1400 V; mass range, *m*/*z* 25−700; N_2 sheath gas, 70 psi; ion source pressure, 800 mTorr; manifold pressure, 5.5 × 10^{-6} Torr; capillary voltage and temperature, 10.9 V and 195 °C; tubel voltage, −3.0 V; and detection in the positive ion mode (MS) and at 214 nm (UV). Data were accumulated in the centroid mode with scans taken every 0.5 s.

The concentration dependent oxidations were analyzed by nonlinear regression with Graph-Pad Prism software (San Diego, CA) and the equations $v = k_{cat}\,S/(K_m + S)$ (Michaelis−Menten equation) and $v = k_{cat}S^n/(S_{50}{}^n + S^n)$, where S represents substrate concentration, S_{50} is the substrate concentration required to reach half-maximal velocity, V_{max} is the maximal velocity, and n is a measure of the cooperativity (*15*). The Michaelis−Menten equation was used when the fits between the equations could not be distinguished, in which case $n = 1$.

Oxidation of αNF. Samples were analyzed by HPLC as described elsewhere (*6*) to idendify αNF oxidation products. The major product (>90%) was previously assigned as the 5,6-oxide on the basis of its parent ion (*m*/*z*) in the mass spectrum and its UV spectrum (*6*, *43*). However, work by others reported two major peaks, one assigned as the 5,6-oxide and the other the 7,8-dihydrodiol, on the basis of comparison of general HPLC profiles with another study (*44*). However, we found only traces of an earlier eluting peak, which is judged to be a dihydrodiol on the basis of its UV spectrum and increased presence in samples containing epoxide hydrolase (and in liver microsomes). The major product was isolated from a preparative microsomal incubation (50 mL) and shown unambiguously to be the 5,6-oxide by its ^1H NMR spectrum ($CDCl_3$, 400 MHz): the expected H-5 and H-6 protons are shifted upfield from their normal positions (*43*) and appear as a pair of doublets with $J = 4.0$ Hz (see Supporting Information).

NADPH Oxidation. Reconstituted P450 3A4 (see P450 Catalytic Activity Assays) was preincubated for 4 min at 37

°C with ligands of interest. The sample was transferred to a 1.0 cm cuvette and the baseline was set to zero. NADPH was then added (10 μL of 10 mM NADPH to give a final of 100 μM) to initiate the reaction and A_{340} was monitored for $\geq$3 min ($\Delta\epsilon_{340}$ = 6.22 mM^{-1} cm^{-1}), which was plotted versus ligand concentration and analyzed by nonlinear regression as described above (see P450 Catalytic Activity Assays).

Reduction Kinetics. Rates of reduction of ferric P450 3A4 were measured under anaerobic conditions in the presence of saturating CO as described elsewhere (*45*). Reconstituted P450 3A4 (as described above; see P450 Catalytic Activity Assays) was diluted to 0.37 μM P450 3A4, 0.73 μM NADPH−P450 reductase, and 0.37 μM cytochrome b_5 in 100 mM potassium HEPES buffer (pH 7.4) with 30 mM $MgCl_2$, 100 IU of glucose oxidase mL^{-1}, 10 μg of catalase mL^{-1}, 120 μM glucose, and ligand of interest as follows: 50 μM or 200 μM testosterone, 5 μM αNF, and/or 10 μM YPFP-NH_2. The sample was made anaerobic under Ar and saturated with CO gas while anaerobic conditions were maintained. The anaerobic sample was then loaded into a stopped-flow device (Applied Photophysics, SX-18MV, Leatherbarrow, U.K.) and combined with an anaerobic CO-saturated solution of NADPH (1.5 mM) in 100 mM potassium HEPES (pH 7.4). Reactions were run at 37 °C with data collection at 448 nm to monitor the formation of the Fe^{2+}·CO complex. Data were analyzed with Graph-Pad Prism software by comparing the fits to monophasic and biphasic exponential reactions.

Spectral Binding Titrations. Purified P450 3A4 was diluted to 1 μM in 100 mM potassium phosphate (pH 7.4) and aliquoted (1.0 mL) into two glass cuvettes. A baseline of the reference cuvette was recorded (350−500 nm) on an Aminco DW-2a/Olis spectrophotometer (On-Line Instrument Systems, Bogart, GA). Ligand was subsequently added and spectra were recorded (350−500 nm) after each addition. The vehicle solvent was added to the reference cuvette (CH_3OH for all ligands except peptides, which were dissolved in H_2O; the final CH_3OH concentration was kept $\leq$2% v/v). For analyses with multiple ligands, the inhibitory ligand of interest was added to the sample cuvette, the baseline was recorded, and the titration was completed as above. The difference in absorbance between the wavelength maximum and minimum was plotted vs the ligand concentration, which was analyzed by nonlinear regression methods with Graph-Pad Prism software. Two equations were compared statistically to determine the best fit: $\Delta A = B_{max}S/(K_s + S)$ and $\Delta A = B_{max}S^n/(K_s^n + S^n)$, where S represents substrate concentration, K_s is the spectral dissociation constant, B_{max} is the maximal binding, and n is a measure of the cooperativity (*15*). The former equation was used when the fits between the equations could not be distinguished, in which case n = 1. Binding titrations with ferrous P450 were completed as above, except that ~1 mg of $Na_2S_2O_4$ was added to the both the reference and sample prior to recording the baseline and a new P450 aliquot was used for each ligand concentration rather than adding the ligand sequentially.

RESULTS

Structure−Affinity Relationships of Peptides. The peptides under consideration interact with the ferric heme iron through a nitrogen on the peptide, as indicated by the type II binding spectra with a decrease in absorbance at 390 nm and an increase in absorbance at 430 nm (Figure 1). The binding affinities (Table 1) for a structural series of the peptides indicated that affinity is enhanced by the addition of a C-terminal amide and the presence of tyrosine at the N-terminus. A further enhancement in affinity, although slight, was seen by the presence of aromatic groups in the interior of the peptide, i.e., Y(D)WGFM-NH_2 compared to YGGFM-NH_2 (met-enkephalin). The free N-terminal nitrogen was imperative for the interaction with the heme iron, as indicated by loss of signal with *N*-acetyl-YPFP-NH_2, and was a major contributing structural feature enhancing affinity. Although an actual K_s could not be obtained with *N*-acetyl-YPFP-NH_2, a K_i for inhibition of testosterone binding was estimated at 670 μM, 100-fold greater than for YPFP-NH_2.

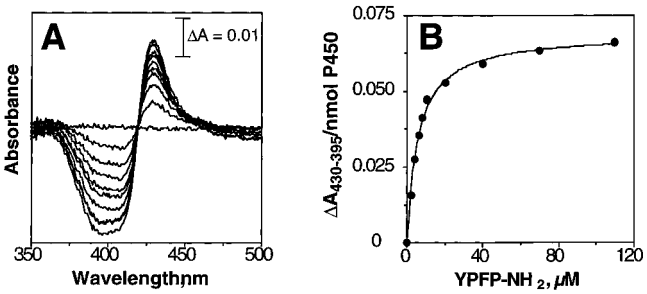

FIGURE 1: Titration of ferric P450 3A4 with YPFP-NH_2. (A) P450 3A4 (1.5 μM) was divided into each of two 1.0 mL glass cuvettes and a baseline was set. Aliquots of YPFP-NH_2 (10 μL of a 50× concentrated stock in H_2O) were added to the sample cuvette and equal volumes of H_2O were added to the reference cuvette. (B) Plot of $\Delta A_{430-395}$ (from panel A) vs concentration of YPFP-NH_2.

Table 1: Binding of Peptides to P450 3A4

peptide	K_s (μM)
YPF	79 ± 4
YPFP	77 ± 3
YPFP-NH_2	7.8 ± 2.4
N-Ac-YPFP-NH_2	*a*
YGG	*b*
YGGF	470 ± 30
YGGFL	360 ± 20
YGGFL-NH_2	15 ± 1
GGFL-NH_2	67 ± 3
GGFL	*a*
YGGFM	300 ± 20
YGGFM-NH_2	12 ± 1
GGFM-NH_2	83 ± 4
GGFM	*b*
YPWG-NH_2	8.8 ± 0.2
Y(D)WGFM-NH_2[c]	7.2 ± 0.4

[a] Spectral signal too low for determination. [b] Peptide solubility too low for determination. [c] D-Trp at second position.

Binding Stoichiometry of Indinavir. The HIV protease inhibitor indinavir has been reported to have high affinity for P450 3A4 (*46*). In that indinavir is "peptidelike," we felt that it might mimic the binding observed with the bioactive peptides and extended our analysis. Binding analysis showed nearly equimolar binding of indinavir to P450 3A4 (Figure 2) as determined by the break in the titration plot. The K_s was set at 0.3 μM to fit the data, yielding a stoichiometry of unity after correction of the amount of the protein by quantitative amino acid analysis.

Cooperativity of P450 3A4-Catalyzed Oxidations. In previous work (*6*) we reported positive cooperativity in the

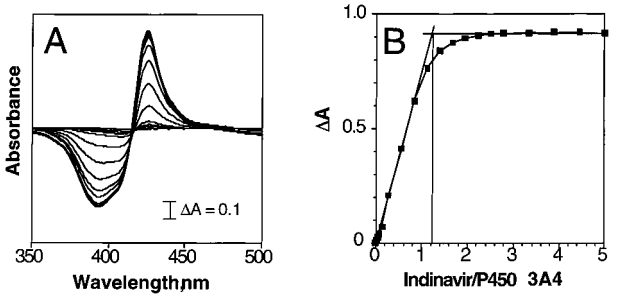

FIGURE 2: Titration of ferric P450 3A4 with indinavir. (A) Spectral changes for P450 3A4 with varying indinavir concentration. The procedure is similar to that described with YPFP-NH_2 in Figure 1, except that the P450 concentration was 18 μM. (B) Plot of $\Delta A_{430-395}$ (from panel A) vs concentration of indinavir. The P450 3A4 concentration indicated on the axis was based upon spectrally determined P450 and not corrected for quantitative amino acid analysis.

Table 2: Catalytic Parameters for Substrate Oxidation

substrate (product in parentheses)	oxidation parameters[a]		
	S_{50} (μM)	k_{cat} (min^{-1})	n
testosterone (6β-OH)	60 ± 13	79 ± 4	1.6 ± 0.1
midazolam			
(1′-OH)	4.6 ± 0.1	2.5 ± 0.6	1.0
(4-OH)	94 ± 16	2.5 ± 0.1	1.0
17β-estradiol (2-OH)	16 ± 1	2.7 ± 0.9	2.0 ± 0.1
αNF (5,6-oxide)	7.8 ± 0.8	6.2 ± 1.5	1.7 ± 0.3

[a] All data were fit to $v = k_{cat}S^n/S_{50}^n + S^n$, where S_{50} is the substrate concentration required to reach half-maximal velocity, and n is an estimate of the extent of cooperativity.

oxidations of testosterone ($n = 1.3$), 17β-estradiol ($n = 1.3$), amitryptiline ($n = 1.4$), and aflatoxin B_1 ($n = 1.8-3.6$). We did experiments with some of these substrates again, because the P450 system had been modified, and found significant positive cooperativity for testosterone 6β-hydroxylation ($n = 1.6$), 17β-estradiol 2-hydroxylation ($n = 2.0$), and αNF 5,6-epoxidation ($n = 1.7$) but not midazolam 1′- or 4-hydroxylation ($n = 1.0$) (Table 2).

Inhibition of Binding of Substrates by YPFP-NH_2. Binding titrations of substrates typically give type I spectra with P450 3A4, indicative of the removal of H_2O as the sixth ligand of the heme iron and resulting in a spin shift of the heme iron from low to high spin (*32*). The spectra are typified by an increase in absorbance at 390 nm and a decrease in absorbance at 420 nm, where the magnitude of the difference of the absorbance maximum and minimum for each particular substrate is assumed to represent the extent of binding to the catalytic site. Binding of testosterone and αNF both gave type I binding characteristics (Figure 3). Furthermore, the binding of these ligands produced sigmoidal binding curves, suggesting that the binding is cooperative (Table 3). Binding of midazolam or 17β-estradiol did not demonstrate cooperative binding, but rather the plots were hyperbolic (Table 3; graphs not shown), suggesting that the sigmoidicity seen with αNF and testosterone is not an experimental artifact.

The difference between YPFP-NH_2, a type II ligand described above, and the type I ligands allows spectral competitive binding titrations for the determination of K_i values and thus affinity of the peptide to a given site (i.e., displacement of peptide by testosterone or another substrate yields a spectral shift, due to displacement of the peptide

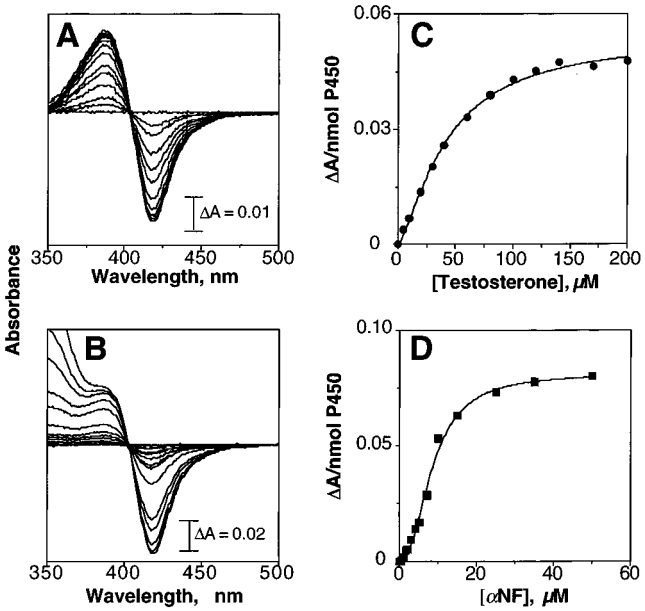

FIGURE 3: Titration of ferric P450 3A4 with (A) testosterone and (B) αNF. The procedure is similar to that described with YPFP-NH_2 in Figure 1. Plots of $\Delta A_{390-420}$ vs (C) testosterone concentration (●) or (D) αNF concentration (■) are also shown.

Table 3: Binding Affinities of P450 3A4 Substrates and K_i Values for YPFP-NH_2 Inhibition of Substrate Binding and Oxidation

substrate (product in parentheses)	substrate binding parameters		inhibition by YPFP-NH_2,[a] K_i (μM)	
	K_s (μM)	n	binding	oxidation
testosterone (6β-OH)	41 ± 11	1.3 ± 0.1	8.2	190
midazolam	8.5 ± 0.2	1.0	7.1	
(1′-OH)				7.5
(4-OH)				180
17β-estradiol (2-OH)	11 ± 1	1.0	*b*	90
αNF (5,6-oxide)	5.7 ± 1.9	1.7 ± 0.4	83	650

[a] All K_i values are competitive. [b] Not determined due to high absorbance background.

type II ligand, with a shift of the spectrum from 430 to 390 nm). The inhibition by YPFP-NH_2 was competitive in nature as indicated by the change in K_s apparent values, with little change in B_{max} values or extent of cooperativity (Figure 4). However, the mechanism of inhibition assumes that the change in signal reflects mutually exclusive binding. The results suggest two distinct binding sites for the peptide YPFP-NH_2, a higher affinity site overlapping with testosterone and midazolam and a lower affinity site overlapping with αNF. Inhibition of 17β-estradiol binding could not be determined due to the high background absorbance. It should be noted that since the binding is cooperative for some of the ligands analyzed, entire concentration-dependent curves were generated for the inhibition by YPFP-NH_2 rather than using a transformation method (e.g., Lineweaver−Burk transformation), which is often nonlinear with sigmoidal data.

Lack of Oxidation of YPFP-NH_2. YPFP-NH_2 (10 or 100 μM final) was incubated with P450 3A4 in the manner used for other substrates. No oxidation was detected by HPLC analysis (A_{215} detection) under a variety of conditions, and the lack of oxidation was confirmed by HPLC/MS with *m*/*z* set for M + 16 (+O) and M − 2 (i.e., M + 16 − 18 = +O, $-H_2O$), plus collection of full spectra. The level of detection

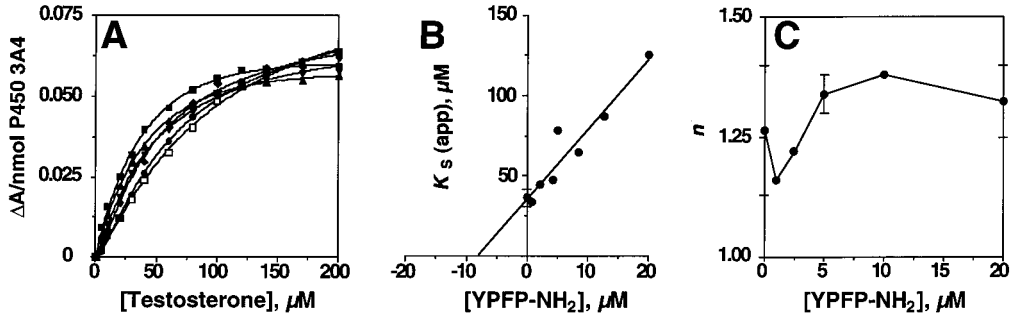

FIGURE 4: Competition of YPFP-NH_2 for testosterone binding to ferric P450 3A4. (A) $\Delta A_{390-420}$ vs testosterone concentration in the absence and presence of varying concentrations of YPFP-NH_2: (■) 0, (▲) 1 μM, (▼) 2.5 μM, (◆) 5 μM, (●) 10 μM, and (□) 20 μM. (B) Plot of K_s (apparent values) vs YPFP-NH_2 concentration: $K_i = 8.2$ μM ($-x$-axis intercept). (C) Plot of n (a measure of extent of cooperativity) vs YPFP-NH_2 concentration.

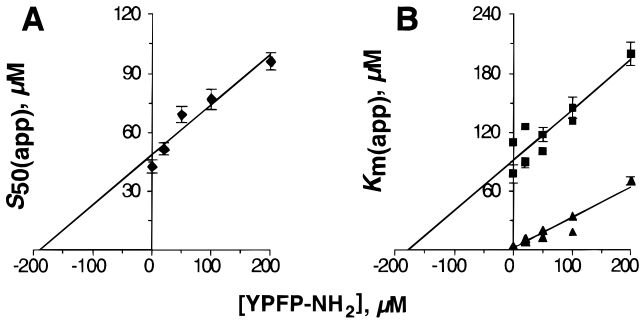

FIGURE 5: Inhibition of P450 3A4-catalyzed (A) testosterone 6β-hydroxylation (◆) or (B) midazolam 1′-hydroxylation (▲) or 4-hydroxylation (■) by YPFP-NH_2. Plots are apparent S_{50} or K_m values vs varying YPFP-NH_2 concentrations, giving the K_i values indicated in Table 3.

corresponded to a rate of <0.1 min^{-1}, based on a conservative estimate and assuming equal ionization properties for YPFP-NH_2 and any products.

Inhibition of Substrate Oxidation by YPFP-NH_2. Inhibition of substrate oxidation catalyzed by P450 3A4 was analyzed to determine K_i values. Although the peptide was not found to be a substrate of P450 3A4, YPFP-NH_2 competitively inhibited catalysis of testosterone, midazolam, 17β-estradiol, and αNF (Table 3) in a manner similar to that observed in the binding analysis, as indicated by effects seen on K_m (S_{50}) and with little or no effect seen on the k_{cat} and n (the extent of cooperativity) (results not shown). However, the K_i values are not similar to the spectral binding assay results (K_s values), with the exception of inhibition of 1′-hydroxylation of midazolam. In theory, the K_i of YPFP-NH_2 inhibition reflects affinity of the peptide to that respective binding site. Formation of the two midazolam products was inhibited with different apparent YPFP-NH_2 affinities (e.g., K_i values), suggesting the presence of different binding sites for midazolam and YPFP-NH_2 (Figure 5).

The difference in inhibitory potential between spectral binding of substrate and catalysis of substrate oxidation was suspected to be due to loss of affinity of YPFP-NH_2 to a different form of the heme iron following reduction by NADPH−P450 reductase. The affinity of YPFP-NH_2 was ∼10-fold less to the ferrous form than to the ferric form of P450 3A4 (K_s 68 vs 7.8 μM, Figure 6).

Influence of Ligand Binding on P450 Reduction Rates. Rates of reduction of P450 3A4 by NADPH−P450 reductase can be stimulated by the presence of substrate (*47*, *48*). Testosterone and αNF stimulated reduction rates to the same extent, with first-order rates of 220 min^{-1} (Figure 7A, spectrum a) and 280 min^{-1} (Figure 7B, spectrum a), respectively, in the presence of ligand as compared to ∼60 min^{-1} in the absence of ligand. When testosterone and αNF were examined in combination, the rate of reduction was further enhanced in an additive manner over the enhancement seen when the ligands were examined individually ($k = 530$ min^{-1}, Figure 7B, spectrum b).

Reduction of P450 3A4 was neither stimulated nor inhibited by YPFP-NH_2 (Figure 7A, spectrum c). Additionally, YPFP-NH_2 did not inhibit the stimulation of the initial reduction rate when examined in combination with testosterone (Figure 7A, spectrum b compared to spectrum a) although a slight reduction in the maximal absorbance was observed. These results are consistent with YPFP-NH_2 not being a substrate of P450 3A4 as determined by lack of product formation (vide supra) and by the lack of stimulation of NADPH consumption (results not presented).

DISCUSSION

Stimulation of P450 3A substrate oxidation reactions by effectors has been known for nearly 25 years, with in vitro and in vivo evidence for both homotropic and heterotropic modulation of oxidations (*6*, *8*, *10*−*14*, *18*, *22*, *24*, *49*, *50*). The mechanism of the modulation of catalytic activity has remained undefined, although several reports provide evidence for an allosteric mechanism. Reports speculate on the binding of multiple ligands to rather distinct allosteric sites (*13*, *51*, *52*) or binding to a large catalytic site that enhances the interaction of the primary substrate to the catalytic site near the heme iron (*19*, *20*, *24*, *53*), while other reports speculate that the allosteric site itself is catalytic (*54*). Absent from the current reports is clear evidence for multiple ligands binding to a single P450 3A4 molecule. We provide evidence in support of such binding utilizing the peptide YPFP-NH_2, which displays high affinity for P450 3A4 yet does not appear to be a substrate. Thus, the peptides offer a tool to study binding without the complication of oxidation.

Evidence for Multiple Ligand Binding Sites. The binding of the peptides resulted in type II binding spectra, which indicate that these ligands are bonded to the heme iron because this type of binding spectrum arises from nitrogen interaction with the iron atom (*32*, *33*). Binding of the typical P450 3A4 substrates, e.g., testosterone and αNF, induces a type I spectrum indicative of displacement of the sixth-ligand H_2O molecule from the heme iron (*32*, *33*). The difference in spectral shifts enabled the analysis of the inhibition of

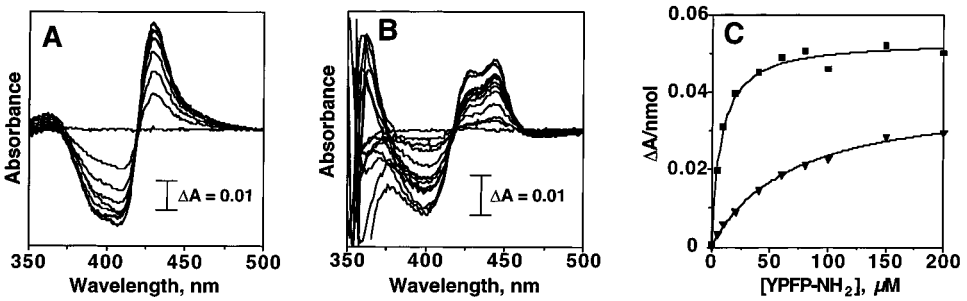

FIGURE 6: Titration of ferrous P450 3A4 with YPFP-NH_2. The procedure is described under Experimental Procedures and is analogous to the work presented in Figure 1, except that $Na_2S_2O_4$-reduced P450 3A4 was used under an Ar atmosphere. Binding titrations of (A) ferric P450 and (B) ferrous P450 generated by addition of $Na_2S_2O_4$; (C) plot of ΔA/nmol of P450 vs YPFP-NH_2 concentration with (■) ferric P450 and (▲) ferrous P450. $K_s = 7.8$ μM for ferric and 68 μM for ferrous P450.

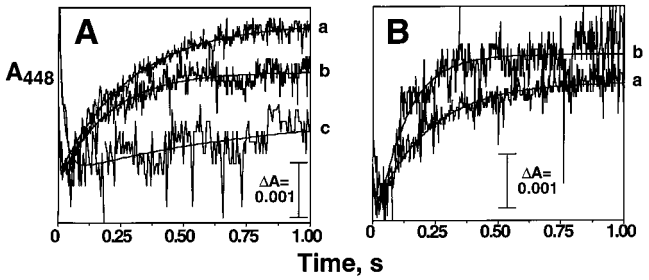

FIGURE 7: Reduction of ferric P450 3A4 under anaerobic conditions and saturating CO in the presence of various ligands: (A) (a) 50 μM testosterone ($k = 220$ min^{-1}), (b) 50 μM testosterone plus 10 μM YPFP-NH_2 ($k = 320$ min^{-1}), and (c) 10 μM YPFP-NH_2 ($k \sim 60$ min^{-1}); (B) (a) 5 μM αNF ($k = 280$ min^{-1}) and (b) 5 μM αNF plus 50 μM testosterone ($k = 530$ min^{-1}).

substrate binding by YPFP-NH_2 (Table 3) and can be interpreted as the confirmation of multiple binding sites. In particular, two sites can be interpreted from the results: a higher affinity site that overlaps with testosterone, midazolam, and possibly 17β-estradiol[2] binding sites and a lower affinity site that overlaps with an αNF binding site.

YPFP-NH_2 also inhibited substrate oxidation in a competitive manner, similarly to observations of substrate binding. Although the affinity of the peptide is substantially less to ferrous P450 compared to ferric P450, the results consistently reveal two main groups of affinity, again supporting the view of two binding sites for the peptide with the lower affinity site overlapping with the αNF oxidation site. There is precedence for individual binding sites for substrates such as testosterone and the classical effector αNF. Although αNF is oxidized to the 5,6-oxide by P450 3A4, the addition of αNF does not have a detectable effect on testosterone oxidation (*6*).

Discrimination of Binding of YPFP-NH_2 to Oxidation States of P450 3A4. The differences in the K_i values of YPFP-NH_2 binding and the steady-state oxidation of substrates (e.g., testosterone, midazolam, and αNF in Table 3) is rationalized in terms of weaker affinity of YPFP-NH_2 for the ferrous than the ferric form of P450 3A4 (Figure 6). An important point can be made here: the two forms of P450 differ in oxidation state and can be considered distinct forms of the enzyme in the same sense that the designations E, E′, etc. are used in considerations of allosteric systems (*55*). Thus, Scheme 1 is proposed to explain the system. Substrate

Scheme 1: Model for Inhibition of P450 3A4 by YPFP-NH_2[a]

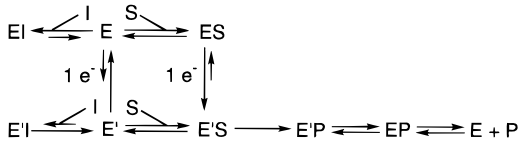

[a] E = P450 Fe^{3+}, E′ = P450 Fe^{2+}, I = YPFP-NH_2 or related peptides, S = testosterone, midazolam, etc.

binds equally well to both enzyme forms (ferric and ferrous) but the inhibitor binds well only to one form (ferric). Thus, substrate will be more competitive with inhibitor when the enzyme is moving through the reaction cycle (including the ferrous enzyme). The ferric and ferrous forms of the P450 may well have different conformations; structural evidence indicates changes in P450s 101 (*56*) and 102 (*57*) upon reduction. In one sense, Scheme 1 is an oversimplification of the situation, since many intermediate forms of P450 exist in the catalytic cycle and each one could be considered a distinct form of the enzyme, perhaps having some conformational identity. However, applying such a rationalization requires that ligand dissociation be faster than the conversion to the next P450 catalytic intermediate. What would a typical k_{off} rate be? If we assume a k_{on} rate of $\sim 10^6$ M^{-1} s^{-1} for association of a protein and ligand, which is generally accepted to be a lower-end value for diffusion-limited enzyme systems (*58*), then a K_d of 10^{-4} M for binding of YPFP-NH_2 to ferrous P450 3A4 yields $k_{off} \sim 10^2$ s^{-1}, or 6×10^3 min^{-1}, which is $\sim 10^2$ faster than the rate-limiting step with P450 3A4 (and probably similar to the rate of O_2 binding at an O_2 concentration of 2×10^{-4} M). Thus, individual intermediates in the P450 catalytic cycle should be considered to be potentially different enzyme forms in consideration of ligand interactions and cooperative phenomena, just as the classic R and S forms of allosteric proteins (*55*).

Another important point to discuss regarding treatment of the ferric and ferrous states (and probably some other catalytic intermediates) as distinct enzyme forms is the acceleration of reduction by substrates (Figure 7). The acceleration of the reduction of P450 3A4 by substrates is seen in most systems (including human liver microsomes) with the exception of baculovirus microsomes in which a large excess of NADPH−P450 reductase has been expressed (*48*). The basis of the stimulation is not known; it does not appear to be thermodynamic because testosterone does not alter the oxidation−reduction potential (*45*). We presume

[2] YPFP-NH_2 binding relative to 17β-estradiol remains inconclusive because the high background of 17β-estradiol absorbance precluded determination of 17β-estradiol in the presence of the peptide (Table 3

Scheme 2: Working Model of P450 3A4

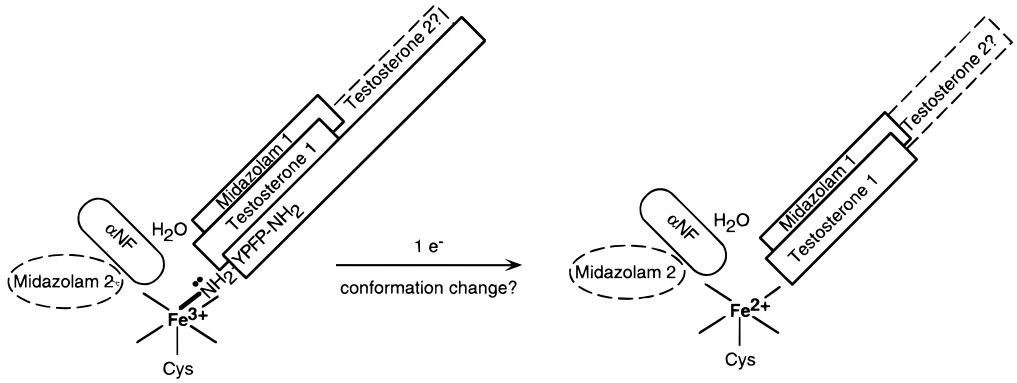

that the binding of substrate to P450 3A4 induces a change in conformation to facilitate electron transfer, but the molecular basis for such a change is unknown. The available evidence with P450s with crystal structures shows conformational changes upon binding of substrate (*58*), although it has not been shown that conformational changes are a prerequisite to substrate oxidation. Interestingly, we have not encountered ligands that stimulate steady-state P450 3A4 oxidation of NADPH without being oxidized, nor have we found substrates that are oxidized but do not stimulate P450 3A4 reduction [although the number of compounds we have examined is limited (*6*); Figure 7]. For example, in this study YPFP-NH_2 was bound to ferric P450 3A4 but neither stimulated reduction nor was oxidized (Figure 7). The interaction of the peptide amino group with the heme iron does not preclude catalysis, because indinavir (Figure 2) is known to be oxidized by P450 3A4 (*59*).

Evidence for a Three-Site P450 3A4 Model. To explain the data from the present studies as well as previous work, we propose a three-site P450 3A4 model as described in Scheme 2. In this scenario testosterone, midazolam, and αNF all produce type I binding spectra (presumably displacing the iron distal H_2O) and also stimulate reduction. The peptide YPFP-NH_2 (M_r 521) best competes for binding in the testosterone$_1$/midazolam$_1$ site, binds via an Fe−N bond, and has considerably reduced affinity for the ferrous enzyme. This loss of affinity may reflect a conformational change in P450 3A4 and not the change in the electronic properties of the iron atom, because other amines are reported to have similar affinities for ferric and ferrous iron (or actually to preferentially bind ferrous iron) (*60*). The low affinity of YPFP-NH_2 for ferrous P450 3A4 cannot by itself explain the lack of oxidation of the peptide because no oxidation was observed even at high concentrations (100 μM). We presume that none of the atoms are in positions appropriate for oxidation. The site labeled testosterone$_2$ is postulated on the basis of the sizes of YPFP-NH_2 and testosterone.

All of the YPFP-NH_2 molecule is considered to bind within P450 3A4 because (i) the observed type II binding spectrum is indicative of Fe−N bonding with the only amino group in the peptide (and *N*-acetylation abolished binding) and (ii) modification at the C-terminus had a strong effect on binding (Table 1). The size occupied by YPFP-NH_2 (M_r 521) is roughly twice that of testosterone (M_r 288) (midazolam M_r 326). Precedence for multiple binding of testosterone molecules exists because homotropic, cooperative binding and kinetics are observed. The titration with indinavir [M_r 614, a known inhibitor (*46*)] revealed one binding site, but the existence of additional "silent" sites cannot be precluded because potential secondary ligand binding may not produce a further absorbance change.

A second site binds αNF. This view is based on the difference in the K_i values of YPFP-NH_2 for blocking αNF and testosterone (Table 3). We cannot rule out the possibility that αNF can also move into the testosterone site, but the results support at least one binding and oxidation site for αNF that is distinct from a testosterone site of interaction. αNF does yield a type I binding spectrum (Figure 3C), so we presume that its binding somehow leads to H_2O displacement from the ferric iron. The point should also be made that αNF binding shows sigmoidicity (Figure 3D), which could be the result of αNF occupancy of the αNF site plus one of the others.

Evidence for the third site arises from analysis of midazolam oxidation in the presence of YPFP-NH_2. The potent inhibition of the 1′-hydroxylation of midazolam by the peptide indicates that YPFP-NH_2 does indeed have a high-affinity site of interaction during the catalytic site that is not seen in the binding spectra with ferrous P450 3A4. Thus, this site is distinct from the site overlapping with testosterone$_1$ and αNF sites of interaction. The view that two sites exist for midazolam binding (midazolam$_1$ and midazolam$_2$) is based on (i) the distinct K_m values for 1′- and 4-hydroxylation (Table 2) and (ii) the distinct K_i values for inhibition of 1′- and 4-hydroxylation of midazolam by YPFP-NH_2 (Table 3). The competitive inhibition of midazolam 1′-hydroxylation by the peptide resulted in a K_i 10-fold less than for YPFP-NH_2 binding to the ferrous form of the enzyme. This result suggests that YPFP-NH_2 indeed has some high-affinity site of interaction during the catalytic cycle (i.e., with the ferrous form of the enzyme). Additionally, αNF has been shown to stimulate midazolam 1′-hydroxylation while having no effect on 4-hydroxylation of midazolam (*23*). If midazolam and αNF have overlapping binding sites with P450 3A4, one would expect modulation through mutually exclusive binding and thus inhibition. The difference in the YPFP-NH_2 K_i values for the midazolam products (Figure 5) is striking and not readily explained without involving multiple modes of midazolam binding. The multiple K_i values for inhibition of the two different oxidations of midazolam by YPFP-NH_2 likely reflect a binding phenomenon; however, kinetic influences in the mechanism of midazolam oxidation cannot be ruled out because little information is available with regard to the meaning of K_m values.

Scheme 3: Alternate Kinetic Explanations for Sigmoidal Responses.[a]

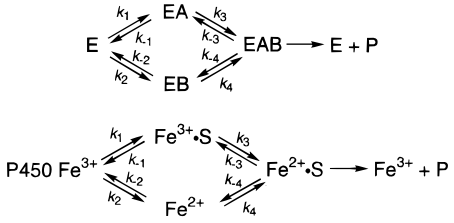

[a] Bi-uni random model (*55, 73*).

Relationship of Current Model to Other P450 3A Proposals. P450 3A enzymes have been studied most extensively in terms of cooperativity but are not the only P450s for which such behavior has been reported. Other P450s, even if not clearly identified, have been reported to show homotropic (*19, 51, 61*) and heterotropic behavior (*10, 62*−*68*). As in the case of many reports of homotropic behavior with P450 3A enzymes, the *n* values (i.e., the extent of positive cooperativity) are usually low. The sigmoidicity is often driven by a small number of measurements, and unfortunately in many cases either plots are not shown or else the analysis does not indicate the error in the estimates of parameters. Another general problem in the area is that analysis through site-directed mutagenesis approaches can provide only limited information, since it is often unclear how to interpret the resulting Hill parameters. The Hill equation describes a phenomenon mathematically, not mechanistically, and thus the parameters do not shed light on the specific nature of cooperativity. An amino acid substitution may have a more global effect, as demonstrated in the recent report of Joo et al. (*69*) where random mutagenesis of P450 101 yielded enzymes with increased catalytic activities due to changes at sites known through crystallographic work to be distant from the substrate binding site.

Another issue in the interpretation of cooperativity is the limited number of studies on binding of ligands. Most of the literature in this area deals only with the interpretation of steady-state kinetic results. The majority of the studies yield partial competitive inhibition with some asymmetries for interactions of two substrates (*6, 18, 25, 26, 49*). Some of the steady-state work has been fit to more complex steady-state models (*19, 54*), but a general concern in these systems is that the only parameters considered are K_m and k_{cat} (often presented as V_{max}) and independent interaction among the multiple sites for binding and oxidation is assumed. The rate-determining steps are not well established in very many P450 systems and the meaning of K_m is usually unknown (*70*); our own work with P450 2E1 (*71, 72*) and the results presented in Table 3 show the complexity of interpretations regarding ligand binding and steady-state kinetic parameters.

The rapid reduction of ferric P450 3A4 in the presence of substrate presents an interesting consideration regarding cooperativity. One model for sigmoidal kinetic response involves ligand complexes, in the absence of a second "allosteric" site (Scheme 3) (*55, 73*). The system is bi-uni random and involves the formation of the complex EAB with both of the substrates bound. There are two possible routes to EAB; one is favored because binding of A provides a kinetic preference for binding B. The thermodynamics are identical for getting to EAB regardless of the path (i.e., $K_1K_3 = K_2K_4$), but $k_1k_3 > k_2k_4$ (*55*). The model could be applied to P450, if we consider B to be an electron (treated here as a substrate). Since binding of substrates facilitates reduction under most conditions (*6*), then $k_1k_3 > k_2k_4$ and sigmoidal kinetics could be expected (*55*). Some of the previous literature (at least some of the homotropic cooperativity) could probably be explained in such terms (*19, 20*).[3] It is also possible that such a model could also explain heterotropic cooperativity if one ligand could bind, facilitate reduction, and exchange at the level of the Fe^{2+}•S complex (vide supra).

Relatively little has been done in terms of analysis of actual binding of ligands to P450 3A, where only the work of Harlow and Halpert (*24*) on the cooperative binding of testosterone was found in the available literature ($n = 1.3$). We also found positive cooperativity in the binding of testosterone ($n = 1.3$) and αNF ($n = 1.7$) (Figure 3). Cooperative binding, which may translate to cooperative oxidation, supports the use of an equation that accounts for interacting binding sites such as the Hill equation employed here (see Experimental Procedures) rather than an equation that assumes lack of interaction and independence of the multiple sites. While the Hill equation may not provide a completely satisfactory solution to analysis of P450 3A4 sigmoidal kinetics, the equation offers a fit of the data (*6, 22, 24, 25*) without introducing additional parameters for which there is a lack of evidence (*19, 54*).

Another point of interest is that no positive heterotropic cooperativity has been detected in P450 systems supported with oxygen surrogates instead of NADPH/O_2 (*6, 23, 50*). These results can be difficult to interpret because an additional reactant is imposed in the active site (albeit relatively small in the case of iodosylbenzene or cumene hydroperoxide). One interpretation of the results is that the cooperativity is related to the process of electron transfer into P450 3A4. Conney and his associates added purified NADPH−P450 reductase to cholate-solubilized rabbit liver microsomes and found that the K_m for added NADPH−P450 reductase was decreased when stimulatory flavonoids were present (*9, 67*). These compounds appeared to exert their stimulatory effects, at least in part, by enhancing the binding of P450 and the reductase. The question arises as to what the parameter K_m for reductase really encompasses—a K_d, electron transfer, or both? In our own work, the fusion of the P450 3A4 and NADPH−P450 reductase proteins did not affect cooperativity (*6*), although it is not proven that electron transfer is only intramolecular in such fusion proteins (*48*). Cooperativity can be dependent upon experimental conditions (*23*), and in our own work with amitriptyline we noted sigmoidicity in a reconstituted system but not liver or baculovirus microsomal systems (the latter of which contained a large excess of NADPH−P450 reductase) (*27*). In the present work, sigmoidal binding was evident in the absence of reconstitution (Figure 3). Although the model of Scheme 3 may explain these data, the findings of cooperativity in binding to ferric P450 (Figure 3) (*24*) argue that reduction may not be the only explanation for cooperativity (if it is at all).

[3] The observation that cooperativity was detected in 17β-estradiol 2-hydroxylation (Table 2) but not binding (Table 3) suggests that binding may not be responsible for the sigmoidal activity plot. An explanation such as that proposed in Scheme 3 cannot be excluded.

Work with a rabbit P450 subfamily 2C protein also showed cooperativity, and Johnson and Vickery used a model ligand to demonstrate that the presence of effectors enhanced the binding of the ligand to the P450 (as revealed by the type II spectral titrations) (*51*, *61*). This model does not appear to apply to the P450 3A4 situations considered here in that testosterone, YPFP-NH_2, and other ligands appear to compete with each other. Unfortunately, it has not been possible to examine the effects of testosterone and αNF on the binding of each other in that they produce the same spectral changes (i.e., type I) (Figure 3).

Another proposal that has been made regarding the cooperativity of P450 3A4 involves equilibrium of multiple protein conformations. Evidence is limited to interpretations offered in explanation of the effects of ligands on rates of Fe^{2+}•CO reassociation following flash photolysis (*52*, *74*). A model involving altered equilibria for P450 3A4 conformations was suggested in some of our own work to explain differing characteristics of the P450 3A4-mediated oxidations of testosterone and ethylmorphine (*47*). The equilibrium of multiple conformations (at each step of the catalytic cycle) modulated by ligands and differing in catalytic properties is an interesting hypothesis that stands in contrast to efforts to develop models in which multiple ligands are docked in a single rigid protein lattice (*22*). Unfortunately, systems with multiple ligands and multiple conformations (related to function) will be very hard to demonstrate structurally.

Conclusions. Our work differs from previous studies on the steady-state kinetic approaches to the cooperativity of P450 3A4 in that we have focused on a peptide ligand that is not oxidized but has effects on activities that can be interpreted in terms of multiple binding sites. Our results provide evidence for a P450 model with at least two sites proximal to the heme and probably three distinct binding sites (or perhaps more appropriately, modes of binding). We do not know exactly where these sites are or their juxtaposition. The work on the altered affinity for the peptide YPFP-NH_2 in different P450 3A4 oxidation−reduction states argues in favor of a dynamic view of P450 3A4−ligand interactions. Exactly what ligand features influence P450 3A4 reduction (by the reductase) and substrate oxidation (and how much they overlap) is not clear. Finally, it must be emphasized that neither our current working model (Scheme 2) nor any others in the literature are very practical in predicting the behavior of new ligands a priori.

ACKNOWLEDGMENT

We thank T. Kawabata for assistance in characterization of αNF 5,6-oxide, I. H. Hanna for advice on construction and purification of $(His)_5$-tagged P450 3A4, M. V. Martin for technical assistance, R. G. Mundkowski for HPLC/MS assistance, M. Voehler for NMR spectra, and particulary M. Delaforge and D. Mansuy for communication of unpublished results with some of these peptides.

SUPPORTING INFORMATION AVAILABLE

A figure showing the ^1H NMR spectrum of αNF oxidation product formed from P450 3A4. This material is available free of charge via the Internet at http://pubs.acs.org.

REFERENCES

1. Palmer, G., and Reedijk, J. (1992) *J. Biol. Chem. 267*, 665−677.
2. Nelson, D. R., Kamataki, T., Waxman, D. J., Guengerich, F. P., Estabrook, R. W., Feyereisen, R., Gonzalez, F. J., Coon, M. J., Gunsalus, I. C., Gotoh, O., Okuda, K., and Nebert, D. W. (1993) *DNA Cell Biol. 12*, 1−51.
3. Guengerich, F. P., Martin, M. V., Beaune, P. H., Kremers, P., Wolff, T., and Waxman, D. J. (1986) *J. Biol. Chem. 261*, 5051−5060.
4. Wrighton, S. A., and Stevens, J. C. (1992) *Crit. Rev. Toxicol. 22*, 1−21.
5. Guengerich, F. P. (1995) in *Cytochrome P450* (Ortiz de Montellano, P. R., Ed.) pp 473−535, Plenum Press, New York.
6. Ueng, Y.-F., Kuwabara, T., Chun, Y.-J., and Guengerich, F. P. (1997) *Biochemistry 36*, 370−381.
7. Cinti, D. L. (1978) *Pharmacol. Ther. 2*, 727−749.
8. Buening, M. K., Fortner, J. G., Kappas, A., and Conney, A. H. (1978) *Biochem. Biophys. Res. Commun. 82*, 348−355.
9. Huang, M. T., Chang, R. L., Fortner, J. G., and Conney, A. H. (1981) *J. Biol. Chem. 256*, 6829−6836.
10. Huang, M. T., Johnson, E. F., Muller-Eberhard, U., Koop, D. R., Coon, M. J., and Conney, A. H. (1981) *J. Biol. Chem. 256*, 10897−10901.
11. Thakker, D. R., Levin, W., Buening, M., Yagi, H., Lehr, R. E., Conney, A. H., and Jerina, D. M. (1981) *Cancer Res. 41*, 1389−1396.
12. Kapitulnik, J., Poppers, P. J., Buening, M. K., Fortner, J. G., and Conney, A. H. (1977) *Clin. Pharmacol. Ther. 22*, 475−485.
13. Schwab, G. E., Raucy, J. L., and Johnson, E. F. (1988) *Mol. Pharmacol. 33*, 493−499.
14. Lee, C. A., Lillibridge, J. H., Nelson, S. D., and Slattery, J. T. (1996) *J. Pharmacol. Exp. Ther. 277*, 287−291.
15. Kuby, S. A. (1991) in *A Study of Enzymes, Vol. I, Enzyme Catalysis, Kinetics, and Substrate Binding*, CRC Press, Boca Raton, FL.
16. Koley, A. P., Buters, J. T. M., Robinson, R. C., Markowitz, A., and Friedman, F. K. (1995) *J. Biol. Chem. 270*, 5014−5018.
17. Koley, A. P., Robinson, R. C., Markowitz, A., and Friedman, F. K. (1995) *Biochemistry 34*, 1942−1947.
18. Wang, R. W., Newton, D. J., Scheri, T. D., and Lu, A. Y. H. (1997) *Drug Metab. Dispos. 25*, 502−507.
19. Korzekwa, K. R., Krishnamachary, N., Shou, M., Ogai, A., Parise, R. A., Rettie, A. E., Gonzalez, F. J., and Tracy, T. S. (1998) *Biochemistry 37*, 4137−4147.
20. Shou, M., Grogan, J., Mancewicz, J. A., Krausz, K. W., Gonzalez, F. J., Gelboin, H. V., and Korzekwa, K. R. (1994) *Biochemistry 33*, 6450−6455.
21. Wang, H., Dick, R., Yin, H., Licad-Coles, E., Kroetz, D. L., Szklarz, G., Harlow, G., Halpert, J. R., and Correia, M. A. (1998) *Biochemistry 37*, 12536−12545.
22. Domanski, T. L., Liu, J., Harlow, G. R., and Halpert, J. R. (1998) *Arch. Biochem. Biophys. 350*, 223−232.
23. Maenpää, J., Hall, S. D., Ring, B. J., Strom, S. C., and Wrighton, S. A. (1998) *Pharmacogenetics 8*, 137−155.
24. Harlow, G. R., and Halpert, J. R. (1998) *Proc. Natl. Acad. Sci. U.S.A. 95*, 6636−6641.
25. Schmider, J., Greenblatt, D. J., Harmatz, J. S., and Shader, R. I. (1996) *Br. J. Clin. Pharmacol. 41*, 593−604.
26. Schmider, J., Greenblatt, D. J., von Moltke, L. L., Harmatz, J. S., and Shader, R. I. (1995) *J. Pharmacol. Exp. Ther. 275*, 592−597.
27. Shaw, P. M., Hosea, N. A., Thompson, D. V., Lenius, J. M., and Guengerich, F. P. (1997) *Arch. Biochem. Biophys. 348*, 107−115.
28. He, Y. A., He, Y. Q., Szklarz, G. D., and Halpert, J. R. (1997) *Biochemistry 36*, 8831−8839.
29. Hummel, J. P., and Dreyer, W. J. (1962) *Biochim. Biophys. Acta 63*, 530−532.
30. Combalbert, J., Fabre, I., Fabre, G., Dalet, I., Derancourt, J., Cano, J. P., and Maurel, P. (1989) *Drug Metab. Dispos. 17*, 197−207.
31. Peyronneau, M. A., Delaforge, M., Riviere, R., Renaud, J. P., and Mansuy, D. (1994) *Eur. J. Biochem. 223*, 947−956.

32. Schenkman, J. B., Remmer, H., and Estabrook, R. W. (1967) *Mol. Pharmacol. 3*, 113−123.
33. Imai, Y., Horie, S., Yamano, T., and Iizuka, T. (1978) in *Cytochrome P-450* (Sato, R., and Omura, T., Eds.) pp 37−135, Academic Press, New York.
34. Delaforrge, M., Bouillé, G., Jaoen, M., and Mansuy, D. (1996) *Exp. Toxic. Pathol. 48/5*, 344.
35. Beaune, P. H., Umbenhauer, D. R., Bork, R. W., Lloyd, R. S., and Guengerich, F. P. (1986) *Proc. Natl. Acad. Sci. U.S.A. 83*, 8064−8068.
36. Gillam, E. M. J., Baba, T., Kim, B.-R., Ohmori, S., and Guengerich, F. P. (1993) *Arch. Biochem. Biophys. 305*, 123−131.
37. Guengerich, F. P., Martin, M. V., Guo, Z., and Chun, Y.-J. (1996) *Methods Enzymol. 272*, 35−44.
38. Omura, T., and Sato, R. (1964) *J. Biol. Chem. 239*, 2370−2378.
39. Shen, A. L., Porter, T. D., Wilson, T. E., and Kasper, C. B. (1989) *J. Biol. Chem. 264*, 7584−7589.
40. Hanna, I. H., Teiber, J. F., Kokones, K. L., and Hollenberg, P. F. (1998) *Arch. Biochem. Biophys. 350*, 324−332.
41. Shimada, T., Misono, K. S., and Guengerich, F. P. (1986) *J. Biol. Chem. 261*, 909−921.
42. Guengerich, F. P. (1994) in *Principles and Methods of Toxicology* (Hayes, A. W., Ed.) pp 1259−1313, Raven Press, New York.
43. Vyas, K. P., Shibata, T., Highet, R. J., Yeh, H. J., Thomas, P. E., Ryan, D. E., Levin, W., and Jerina, D. M. (1983) *J. Biol. Chem. 258*, 5649−5659.
44. Andries, M. J., Lucier, G. W., Goldstein, J., and Thompson, C. L. (1990) *Mol. Pharmacol. 37*, 990−995.
45. Yamazaki, H., Johnson, W. W., Ueng, Y.-F., Shimada, T., and Guengerich, F. P. (1996) *J. Biol. Chem. 271*, 27438−27444.
46. Inaba, T., Fischer, N. E., Riddick, D. S., Stewart, D. J., and Hidaka, T. (1997) *Toxicol. Lett. 93*, 215−219.
47. Yamazaki, H., Ueng, Y.-F., Shimada, T., and Guengerich, F. P. (1995) *Biochemistry 34*, 8380−8389.
48. Guengerich, F. P., and Johnson, W. W. (1997) *Biochemistry 36*, 14741−14750.
49. Ludwig, E., Schmid, J., Beschke, K., and Ebner, T. (1999) *J. Pharmacol. Exp. Ther. 290*, 1−8.
50. Lee, C. A., Manyike, P. T., Thummel, K. E., Nelson, S. D., and Slattery, J. T. (1997) *Drug Metab. Dispos. 25*, 1150−1156.
51. Johnson, E. F., Schwab, G. E., and Vickery, L. E. (1988) *J. Biol. Chem. 263*, 17672−17677.
52. Koley, A. P., Buters, J. T. M., Robinson, R. C., Markowitz, A., and Friedman, F. K. (1997) *J. Biol. Chem. 272*, 3149−3152.
53. Shet, M. S., Fisher, C. W., Holmans, P. L., and Estabrook, R. W. (1993) *Proc. Natl. Acad. Sci. U.S.A. 90*, 11748−11752.
54. Shou, M., Mei, Q., Ettore, M. W., Jr., Dai, R., Baillie, T. A., and Rushmore, T. H. (1999) *Biochem. J. 340*, 845−853.
55. Segel, I. H. (1975) in *Enzyme Kinetics: Behavior and Analysis of Rapid Equilibrium and Steady-State Enzyme Systems*, pp 460−461, Wiley-Interscience, New York.
56. Poulos, T. L., Cupp-Vickery, J., and Li, H. Y. (1995) in *Cytochrome P450: Structure, Mechanism, and Biochemistry* (Ortiz de Montellano, P. R., Ed.) pp 125−150, Plenum Press, New York.
57. Modi, S., Sutcliffe, M. J., Primrose, W. U., Lian, L.-Y., and Roberts, G. C. K. (1996) *Nat. Struct. Biol. 3*, 414−417.
58. Mueller, E. J., Loida, P. J., and Sligar, S. G. (1995) in *Cytochrome P450: Structure, Mechanism, and Biochemistry* (Ortiz de Montellano, P. R., Ed.) pp 83−124, Plenum Press, New York.
59. Chiba, M., Hensleigh, M., and Lin, J. H. (1997) *Biochem. Pharmacol. 53*, 1187−1195.
60. Cotton, F. A., and Wilkinson, G. (1980) *Advanced Inorganic Chemistry*, pp 755−759, Wiley-Interscience, New York.
61. Johnson, E. F., Schwab, G. E., and Dieter, H. H. (1983) *J. Biol. Chem. 258*, 2785−2788.
62. Wiebel, F. J., Leutz, J. C., Diamond, L., and Gelboin, H. V. (1971) *Arch. Biochem. Biophys. 144*, 78−86.
63. Baker, M. T., Bates, J. N., and Leff, S. V. (1987) *Anesth. Analg. 66*, 1141−1147.
64. Baker, M. T., and Ronnenberg, W. C., Jr. (1992) *Toxicol. Appl. Pharmacol. 114*, 25−30.
65. Wang, Y., Olson, M. J., and Baker, M. T. (1993) *Biochem. Pharmacol. 46*, 87−94.
66. Baker, M. T., Olson, M. J., Wang, Y., Ronnenberg, W. C., Jr., Johnson, J. T., and Brady, A. N. (1995) *Drug Metab. Dispos. 23*, 60−64.
67. Miller, M. S., Huang, M. T., Jeffrey, A. M., and Conney, A. H. (1983) *Mol. Pharmacol. 24*, 137−145.
68. Wolff, T., and Guengerich, F. P. (1987) *Biochem. Pharmacol. 36*, 2581−2588.
69. Joo, H., Lin, Z. L., and Arnold, F. H. (1999) *Nature 399*, 670−673.
70. Northrop, D. B. (1998) *J. Chem. Educ. 75*, 1153−1157.
71. Bell, L. C., and Guengerich, F. P. (1997) *J. Biol. Chem. 272*, 29643−29651.
72. Bell-Parikh, L. C., and Guengerich, F. P. (1999) *J. Biol. Chem. 274*, 23833−23840.
73. Jensen, R. A., and Trentini, W. C. (1970) *J. Biol. Chem. 245*, 2018−2022.
74. Koley, A. P., Robinson, R. C., Markowitz, A., and Friedman, F. K. (1997) *Biochem. Pharmacol. 53*, 455−460.

BI992765T